Time-dependent Hartree-Fock studies of the sensitivity of dynamical fusion thresholds to the effective two-body interaction

J. A. Maruhn
Institut für Theoretische Physik der Universität Frankfurt, Frankfurt, Federal Republic of Germany and Physics Division, Oak Ridge National Laboratory, Oak Ridge, Tennessee 37831

K. T. R. Davies and M. R. Strayer
Physics Division, Oak Ridge National Laboratory, Oak Ridge, Tennessee 37831
(Received 9 November 1984)

Results are presented for time-dependent Hartree-Fock calculations of mostly head-on collisions of $^{86}Kr+^{139}La$ and $^{16}O+^{16}O$. These studies demonstrate the sensitivity of the time-dependent Hartree-Fock dynamical fusion thresholds to the effective two-body interaction used in the calculations. The main thrust of this paper is to investigate the dynamical threshold which is the microscopic analog of the macroscopic extra-push threshold. We find that, for head-on collisions at bombarding energies above the interaction barrier, the onset of fusion is extremely sensitive to the interaction used. The thresholds calculated with different Skyrme forces differ by several hundreds of MeV or more, and are related to the effective mass of the interaction. We also show that the high-energy angular momentum window threshold has a pronounced force dependence, a feature which must be properly taken into account in comparing time-dependent Hartree-Fock window predictions with experimental data. Finally, it is shown that the fusion behavior can be sensitive both to the numerical time step used and to the precision of the calculation, a problem which may have implications regarding the validity of the time-dependent Hartree-Fock results after time scales of the order of 10^{-20} s.

I. INTRODUCTION

There has been great interest in recent years in studies of dynamical thresholds which govern fusion behavior in heavy-ion reactions.[1–20] Two such thresholds can be identified. The first is the low-energy threshold which is associated with the phenomenon known in macroscopic studies as the extra push (or, in some cases, the extra-extra push).[2–4] This threshold can be characterized as follows. For head-on collisions of sufficiently light systems, fusion occurs for center-of-mass (c.m.) bombarding energies greater than or equal to the interaction barrier height. However, for a fixed c.m. energy, if one increases the repulsive potential energy of the system, by increasing the charges of the target or projectile (or the orbital angular momentum), fusion becomes less probable. Thus, e.g., for head-on collisions of a system exceeding a critical fissility,[1–6,19,20] fusion will not occur unless the c.m. energy exceeds the barrier height by a certain threshold value known as the extra-push energy. This threshold occurs theoretically in both macroscopic[1–7,19,20] and microscopic[9,10,15–17,20] studies and its existence is well established experimentally.[3,4,6]

The second type of dynamical threshold occurs only in time-dependent Hartree-Fock (TDHF) calculations at relatively high energies,[9–16,20] where it is found that fusion abruptly disappears for head-on collisions. This threshold is known as the TDHF angular momentum window. For energies above this threshold there exists a low-angular-momentum cutoff below which there is no fusion. This behavior is intimately associated with the transparency inherent in the mean-field approximation and its existence is thought to be very questionable experimentally.[21] This paper will primarily be devoted to studies of the microscopic analog of the macroscopic extra-push threshold, although we will present some results for the window threshold.

It has recently been demonstrated that the extra-push threshold is very sensitive to certain details of the models.[5,6,16,19,20] In a macroscopic study[6,19,20] this threshold was shown to depend strongly on the type of viscosity assumed. Also, a TDHF study[16,20] demonstrated a pronounced sensitivity to the two-body effective interaction used. There is a connection between these macroscopic and microscopic results since both are associated with dissipation. In the TDHF approximation, dissipation arises solely from one-body collisions with the mean-field potential which is, in turn, generated by the two-body interaction. However, we emphasize that the mechanism of dissipation is different in the TDHF approximation than in any of the one-body macroscopic viscosity models.[19]

Of course, in the TDHF approximation the basic behavior depends on the two-body interaction which contains the only adjustable parameters. These parameters are usually fitted to static, low-energy nuclear properties without any regard to heavy-ion dynamical phenomenology. Therefore, it is difficult *a priori* to assess how a change in the interaction will influence the description of heavy-ion collisions. By comparing TDHF results with experiment, one hopes to be able to relate heavy-ion scattering to well-defined properties of the force, e.g., the

incompressibility, effective mass, or surface tension.

During the last eight years, a large number of TDHF calculations have been performed for a variety of heavy-ion reactions,[8–10] and it has become well established now that the calculated TDHF fusion behavior is very sensitive to the effective two-body interaction used. In particular, both the fusion cross sections[9,10,12,22,23] and the angular momentum window threshold[9–12] can depend strongly on the parameters of the force. Recent studies have reported[16,20] that in the $^{86}Kr + ^{139}La$ system the extra-push thresholds for the Skyrme II and Skyrme III interactions differ by more than 250 MeV in laboratory bombarding energy. The main purpose of this paper is to continue and extend these calculations of the $^{86}Kr + ^{139}La$ system, using additional Skyrme forces in order to make a comprehensive study of the force dependence of the extra-push threshold. We will show that the behavior of this threshold can be correlated with the effective mass ratio,[24] m^*/m, of the force. In particular, we find that, as the m^*/m value increases, the system fuses more easily at lower bombarding energies.

The basic outline of the remainder of this paper is as follows. In Sec. II we give a description of the scope of the calculations and the methods used. In Sec. III we present the results of the extra-push threshold studies of $^{86}Kr + ^{139}La$ using different Skyrme forces. In this section we also include some results for both $^{86}Kr + ^{139}La$ and $^{16}O + ^{16}O$ showing the sensitivity to the force of the high-energy angular momentum window threshold, and we present studies of $^{86}Kr + ^{139}La$ for relatively small impact parameters, in which we investigate the force dependence of deep-inelastic scattering for large angle events.[25] In Sec. IV we briefly summarize our results. Finally, we include an Appendix which demonstrates the sensitivity of the fusion behavior to both the numerical time step used and precision of the calculation.

II. CALCULATIONAL DETAILS

Since we are primarily concerned with the onset of fusion for low energies above the barrier and for the disappearance of fusion at higher energies, almost all of our calculations are for head-on collisions of $^{86}Kr + ^{139}La$ and $^{16}O + ^{16}O$. We used the rotating frame, axially symmetric code described in Ref. 8, which exactly reproduces the results from a three-dimensional calculation for zero angular momentum reactions.[26] With this code, we also performed a few calculations of $^{86}Kr + ^{139}La$ for non-head-on collisions in order to examine the force dependence of deep-inelastic scattering for large-angle events.[25] For the $^{86}Kr + ^{139}La$ system, we used a mesh spacing of 0.55 fm, and the main results were obtained using a time step of 0.002×10^{-21} s, with the calculations performed in double precision on the IBM 3033 at Gesellschaft für Schwerionenforschung (GSI). (In the Appendix we report on some additional $^{86}Kr + ^{139}La$ studies using single precision and time steps of 0.01×10^{-21}, 0.005×10^{-21}, and 0.001×10^{-21} s.) For the $^{16}O + ^{16}O$ system, we used a mesh spacing of 0.40 fm and a time step of 0.0025×10^{-21} s, with the calculations performed on the IBM 3033 at the Oak Ridge National Laboratory (ORNL).

Previously the $^{86}Kr + ^{139}La$ system was extensively studied in the TDHF approximation[15,16,25] using Skyrme force II.[27] In Ref. 16 a single calculation of this system was also done using Skyrme force III,[28] in which it was demonstrated that the fusion behavior is dramatically different for these two forces. In the present work we continue these studies of the fusion behavior, comparing results for Skyrme forces II, III, IV, V, and VI.[27,28] The parameters and nuclear matter properties of these forces are listed in Table I. All of the Skyrme forces used in this paper were modified to include the effects of a sum of direct folded Yukawa interactions as described in Refs. 8, 29,

TABLE I. Parameters and nuclear matter properties of the Skyrme potentials used in this paper. Skyrme II is obtained from Ref. 27, while forces III–VI are obtained from Ref. 28. The definitions of the parameters t_0, x_0, t_1, t_2, and t_3 are given in Refs. 24, 27, and 28. The nuclear matter quantities k_F, a_v, a_s, a_τ, K_∞, and m^*/m are, respectively, the equilibrium Fermi momentum, volume energy, surface energy, symmetry energy, compressibility, and effective mass ratio.

Skyrme force	II	III	IV	V	VI
Parameters					
t_0 (fm^3 MeV)	−1169.9	−1128.8	−1205.6	−1248.3	−1101.8
x_0	0.34	0.45	0.05	−0.17	0.583
t_1 (fm^5 MeV)	585.6	395.0	765.0	970.6	271.7
t_2 (fm^5 MeV)	−27.1	−95.0	35.0	107.22	−138.33
t_3 (fm^6 MeV)	9331.1	14000.0	5000.0	0.0	17000.0
Nuclear matter coefficients					
k_F (fm^{-1})	1.30	1.29	1.31	1.32	1.29
a_v (MeV)	−16.00	−15.87	−15.98	−16.06	−15.77
a_s (MeV)	19.92	18.64	19.30	19.80	17.88
a_τ (MeV)	34.16	28.16	28.31	32.88	26.85
K_∞ (MeV)	342.0	356.0	325.0	306.0	364.0
m^*/m	0.58	0.76	0.47	0.38	0.95

and 30. These Yukawa interactions simulate the finite range of the nuclear force and also help to improve the stability of the finite difference algorithm.[8] The calculations do not include spin but do take into account differences between neutrons and protons, with the exchange part of the Coulomb energy computed using the Slater approximation.[31] The present version of the code has not yet been generalized to include the special three-body terms in the Skyrme M interaction[32] and modified Skyrme M interaction,[33] although calculations with these improved potentials are planned for the future.

For the head-on collisions of the $^{86}Kr + ^{139}La$ system, the laboratory bombarding energies used ranged from 370.0 MeV, which is somewhat above the macroscopic interaction barrier, to 830.0 MeV. These calculations were carried out at intervals of roughly 40 MeV.

In the Appendix, we present the results of an investigation of the numerical accuracy of the TDHF calculations. This study shows that the long-time TDHF results *may* only be reliable for a physical time of 5×10^{-21} s or less. Thus, our operational definition of fusion is that, during the reseparation phase, the rms radius of the system reaches a pronounced maximum value after which it decreases.[12,23] Fortunately, for all fusion cases studied, the system remained coalesced for at least 5×10^{-21} s once it had survived the first attempt at reseparation. In practice then, we obtain the same fusion behavior as in a previous study[16] in which the coalesced system was monitored for a much longer time. For long-lived configurations at bombarding energies close to the interaction barrier, reseparation sometimes results from a dynamically metastable situation, in which the motion of a sufficient number of nucleons happens to get in phase and drive the system to fission. It is highly unlikely that any numerical treatment will be able to predict the details of such a process with confidence. What can be said with certainty is only that the system remains in a highly fissionable configuration, and whether in reality it will then finally fission or become a fused system also depends on the dissipation mechanisms neglected in TDHF. As this situation occurs only relatively rarely and near the thresholds for fusion, its only practical effect is to increase the uncertainty in the threshold energies.

III. RESULTS

A. $^{86}Kr + ^{139}La$

We first present our results for the fusion behavior of $^{86}Kr + ^{139}La$. These studies show that the fusion thresholds are very sensitive to the two-body effective interaction used. Figures 1 and 2, for head-on collisions, illustrate how the dynamical behavior depends upon the interaction. In Fig. 1, we display the rms radius of the total system as a function of time for $E_{lab}=370.0$ MeV for the five Skyrme forces considered. The general behavior shown in this figure is similar to that obtained at other energies. The initial minimum of the rms radius depends strongly on the force. Then the smaller the value of this minimum, the more likely the system is to fuse. For Skyrme forces II, IV, and V the initial coalesced system

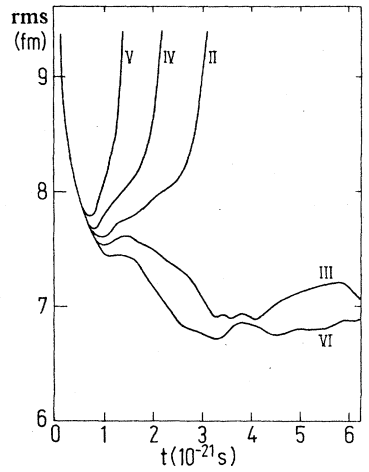

FIG. 1. The rms radius of the total system as a function of time for head-on collisions of $^{86}Kr + ^{139}La$ at $E_{lab}=370.0$ MeV. The roman numeral on each curve labels the Skyrme force used.

clearly reseparates, while it is our interpretation that the reactions for Skyrme forces III and VI lead to true compound nucleus formation (see Sec. II). Thus, the tendency to fuse decreases according to the following sequence of Skyrme forces: VI, III, II, IV, and V.

Figure 2 displays the rms radius as a function of time for Skyrme forces II and III at the higher laboratory bombarding energy of 505.0 MeV.[16] Note, in this figure, that the dynamical behavior is followed for a longer time than that shown in Fig. 1. At $E_{lab}=505.0$ MeV the rms radius for both forces reaches a minimum at roughly 6.4 fm, with the Skyrme III value slightly smaller than the Skyrme II value. The minimum in Fig. 2 is considerably

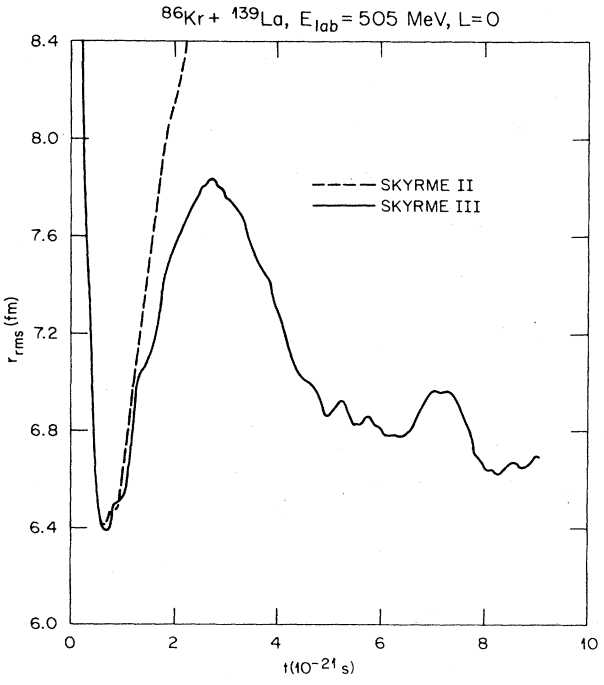

FIG. 2. The rms radius of the total system as a function of time for head-on collisions of $^{86}Kr + ^{139}La$ at $E_{lab}=505.0$ MeV.

smaller than the minima shown in Fig. 1 because the higher energy in Fig. 2 causes the nuclei to interpenetrate more deeply. In Fig. 2, after the Skyrme II radius reaches its minimum, it increases indefinitely as the system reseparates with an energy loss of about 118 MeV.[16] On the other hand, after the rms radius for Skyrme III decreases to its minimum, it then increases to a maximum, after which it is dramatically damped in a highly coalesced state. Thus, for a head-on collision at $E_{\rm lab}=505.0$ MeV, the reaction for Skyrme II gives rise to a deep-inelastic event while that for Skyrme III leads to a fusion. In Figs. 3 and 4, we display the evolution of the density contours at $E_{\rm lab}=505.0$ MeV for the Skyrme II and III potentials, respectively.

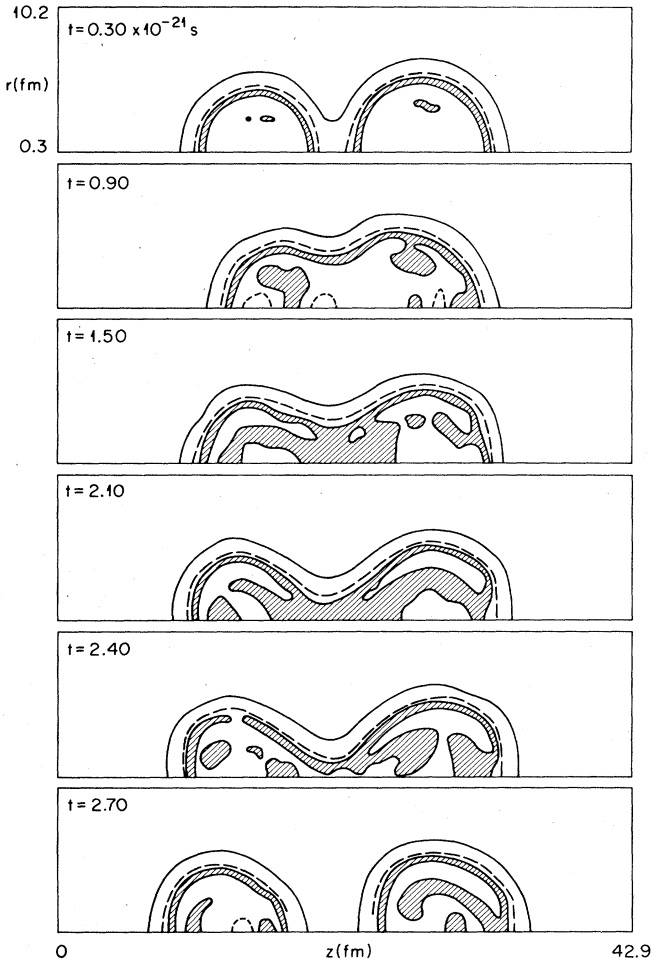

FIG. 3. Equidensity contours at various times during head-on collision of ^{86}Kr + ^{139}La at $E_{\rm lab}=505.0$ MeV for the Skyrme II potential. In each frame the abscissa (z axis) lies along the line joining the mass centers of the projectile and target. The axially symmetric density is plotted as a function of the cylindrical coordinates z and r (ordinate). The two outermost contour lines correspond to mass densities of 0.02 and 0.09 nucleons/fm^3; the shaded region represents densities between 0.12 and 0.14 nucleons/fm^3; and, when present, the innermost (short-dashed) contour line borders a region in which the density is greater than 0.16 nucleons/fm^3. The times are in units of 10^{-21} s.

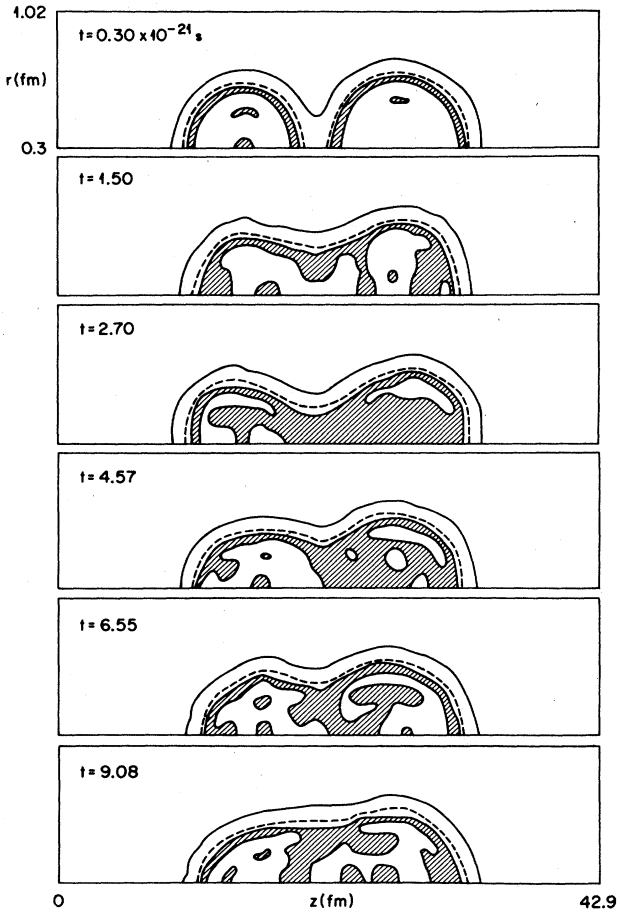

FIG. 4. Equidensity contours at various times during a head-on collision of ^{86}Kr + ^{139}La at $E_{\rm lab}=505.0$ MeV for the Skyrme III potential. See the caption to Fig. 3 for a description of the density contours.

We summarize the results for our fusion threshold studies in Table II and Fig. 5. The error bars in Fig. 5 show the uncertainties in determining the calculated thresholds as indicated in Table II. For example, for the extra-push threshold of Skyrme II, the highest calculated energy for which fusion does not occur is 630.0 MeV and the lowest energy for which fusion does occur is 660.0 MeV. Thus, the precise threshold lies somewhere between these two limits. Also, some comments should be made regarding the blanks inserted for some of the limits listed in Table II. The calculations were performed in the laboratory energy range from 370.0 to 830.0 MeV. The lower energy limit was chosen because it is somewhat above the macroscopic interaction barrier, and we did not exceed the upper limit due to our concern both about numerical instability and about possible important corrections to TDHF at higher energies.[34] Then, for Skyrme forces III and VI, there is essentially no extra-push energy required since fusion occurs for all energies down to the interaction barrier. On the other hand, for Skyrme V, there is a large extra-push energy since the fusion threshold lies between 790.0 and 830.0 MeV. This demonstrates that the extra-

TABLE II. Summary of the maximum and minimum laboratory bombarding energies, in MeV, for which fusion is obtained in head-on collisions of $^{86}Kr + ^{139}La$. The calculated limits for both the extra-push threshold and the window threshold are listed for different Skyrme forces. The calculations for Skyrme forces III—VI were performed in the laboratory energy range from 370.0 to 830.0 MeV. The results for Skyrme II are from Ref. 16.

Skyrme force	II	III	IV	V	VI
Extra-push threshold					
Highest energy giving no fusion	630.0		670.0	790.0	
Lowest energy giving fusion	660.0	370.0	710.0	830.0	370.0
Window threshold					
Highest energy giving fusion	840.0	790.0	830.0		830.0
Lowest energy giving no fusion	850.0	830.0			

push thresholds for different Skyrme forces can differ by almost 500 MeV. Also, for Skyrme forces IV and VI, after fusion occurs at lower energies it continues up to 830.0 MeV, and no window threshold was determined. Table II shows that for Skyrme V fusion begins at 830.0 MeV so that only the extra-push threshold occurs in the energy range under consideration.

For nonfusion reactions at energies below the extra-push threshold (e.g., Skyrme forces II and IV), one observes reflection, with the Kr-like ion appearing to bounce off of the La-like ion.[9,10,15,16] On the other hand, for nonfusion reactions at energies above the window threshold (e.g., Skyrme forces II and III), one observes the usual TDHF transparency effect, with the Kr-like ion appearing to pass through the La-like ion.[9,10,15,16]

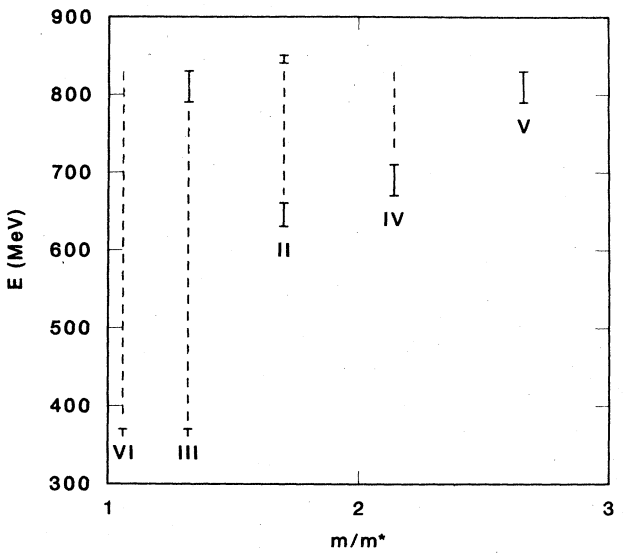

FIG. 5. Dynamical TDHF fusion thresholds for head-on collisions of $^{86}Kr + ^{139}La$. The laboratory energy thresholds for different Skyrme forces are plotted as a function of the inverse of the effective mass ratio (Ref. 24), m/m^*. The error bars indicate the uncertainties in determining the threshold (see Table II). The lower error bars denote the extra-push fusion threshold, while the upper error bars, when present, indicate the window threshold. The dashed lines joining the lower and upper error bars denote the fusion region. The roman numerals label the Skyrme forces.

Figure 5 shows that the extra-push threshold depends very strongly on the Skyrme force used and that this behavior can be correlated with the effective mass ratio of the interaction.[24] We see that as the m^*/m value increases, the system fuses more easily at lower bombarding energies. For the $^{86}Kr + ^{139}La$ system, it appears that the TDHF angular momentum window threshold also varies according to the force used. However, because the window thresholds for three of the potentials are unknown, the force dependence of the window has not yet been well determined for this system.

To complete the studies of the $^{86}Kr + ^{139}La$ system, we investigated the scattering behavior for small but nonzero impact parameters for Skyrme III at $E_{lab} = 505.0$, 610.0, and 710.0 MeV, the three energies where experimental data[35] are available. Previous TDHF studies of both $^{86}Kr + ^{139}La$ (Ref. 25) and $^{84}Kr + ^{209}Bi$ (Ref. 8) showed that the small L, large angle events for the Skyrme II potential are about 50 MeV above the ridge in the experimental Wilczynski plot. Since Skyrme III has a very different fusion behavior for head-on collisions than does Skyrme II, it might be expected that the deep-inelastic scattering behavior might also be modified. However, our studies with Skyrme III, at the smallest angular momenta where fusion does not occur, indicate that the energy loss increases only by about 5—10 MeV compared to Skyrme II. Thus, the large angle discrepancy with the experimental data cannot be eliminated by changing the force. It should be mentioned though that, in comparing the experimental and theoretical results, there are some ambiguities which need to be more carefully understood before this question can definitely be settled.[8]

B. $^{16}O + ^{16}O$

The force dependence of the window threshold for the $^{16}O + ^{16}O$ system has been carefully investigated. The results are presented in Table III, in which we list the opening of the window for different Skyrme forces. The numbers in Table III are in good agreement with the results obtained by Dhar and Nilsson.[11] The force labeled BGK was a very simplified Skyrme force used in the paper of Bonche, Grammaticos, and Koonin.[22] For the other Skyrme forces, the error bars on the threshold energies indicate the precision with which the fusion window has been determined. Notice that there are rather large differences in the various threshold energies, ranging from 42.5 MeV for Skyrme IV to 62.5 MeV for Skyrme II. We emphasize that it is important to eventually study the window for nonzero impact parameters at energies above the threshold. Such studies will help to determine how rapidly the window grows with *both* energy and angular momentum for different forces. Also, it should be pointed out that the experiment of Lazzarini *et al.*[21] was done at a laboratory energy of 68 MeV, which is only 3—8 MeV above the limits for the Skyrme II threshold. Since the results of these measurements seemed to rule out the existence of the window, it is suggested that it might be desirable to do this experiment at a somewhat higher energy.

IV. SUMMARY

TDHF studies of head-on collisions of $^{86}Kr + ^{139}La$ and $^{16}O + ^{16}O$ show a pronounced sensitivity of fusion thresholds to the two-body effective interaction used. Of particular significance is the force dependence of the microscopic analog of the macroscopic extra-push threshold. In the calculations of $^{86}Kr + ^{139}La$ we find that the onset of fusion can vary by hundreds of MeV for different Skyrme forces. For example, the extra-push thresholds for the Skyrme III and V potentials differ by about 450 MeV. Also, this force dependence can be correlated with the nuclear matter effective mass ratio of the potential. We have shown that, as the m^*/m value increases, fusion more readily occurs at lower bombarding energies, so that the extra-push energy threshold increases according to the following ordering of the Skyrme forces: VI, III, II, IV, and V. This force dependence is very likely intimately related to the sensitivity of the macroscopic extra-push results to the type of viscosity assumed.[6,19,20]

Finally, studies of both $^{86}Kr + ^{139}La$ and $^{16}O + ^{16}O$ demonstrate that the relatively high-energy, angular momentum window threshold exhibits a pronounced force dependence. In particular, for $^{16}O + ^{16}O$ the thresholds for Skyrme II and IV differ by 20 MeV, with the threshold for Skyrme II only a few MeV below the energy used in the experiment,[21] which seemed to rule out the existence of the window. We suggest that it would be desirable to reanalyze the experimental and theoretical information, taking into account more carefully the force dependence of the window threshold.

TABLE III. THDF studies of the fusion angular momentum window for head-on collisions of $^{16}O + ^{16}O$. The uncertainty in determining the thresholds is also listed.

Skyrme force	Laboratory threshold energy (in MeV) for the window
BGK (Ref. 22)	54
II	62.5±2.5
III	57.5±2.5
IV	42.5±2.5
V	52.5±2.5
VI	52.5±2.5

ACKNOWLEDGMENTS

We are very grateful to the Gesellschaft für Schwerionenforschung computation center where most of the results of this paper were obtained. We also thank Keh-Fei Liu for helpful discussions concerning the effective mass dependence of the Skyrme forces. This research was sponsored in part by the Division of Nuclear Physics, U.S. Department of Energy under Contract No. DE-AC05-840R21400 with Martin Marietta Energy Systems, Inc.

APPENDIX: NUMERICAL ACCURACY OF THE TDHF SOLUTIONS

A. General remarks

We wish to study the time scale over which the TDHF approach is valid in a heavy-ion collision. Of course, there is always the more general problem of how accurately we are able to solve even the TDHF model in itself. Special attention should be paid to the fact that we are dealing with a time-dependent solution, where errors may accumulate indefinitely. This behavior should be contrasted with a static Hartree-Fock (HF) calculation, in which errors arising in the wave function during the interaction should be eliminated by later iteration until one obtains the best approximation to the true solution possible within well-defined numerical conditions, e.g., mesh spacing and total size for the finite difference grid. On the other hand, in a time-dependent situation the numerical solution may slowly deviate from the true one and the two may become completely different for finite times (unless special circumstances, such as quasiperiodicity, intervene). Such an effect was seen in Ref. 16, where it was found that a change in the time step resulted in a very different total interaction time. Also, there is the possibility of instability; i.e., a difference, initially small, between two solutions may suddenly grow very rapidly with time.

For these reasons, we deemed it necessary to further investigate this problem in detail. We attempted to answer the following question: With a given numerical procedure, and for a fixed set of parameters (like time and space steps), for what length of time can the numerical solutions be trusted in the sense of being reasonably close to the true solution? We will call this time span the "confidence time" of the calculation.

It is clear that in practice this problem can be studied

only via convergence tests. Since these are particularly expensive, the conclusions given in this Appendix will not be exhaustive. We believe, though, that the results obtained are of great significance and indicate where more work remains to be done. We emphasize, too, that our conclusions are strictly valid only for the Peaceman-Rachford method described in Refs. 8 and 36 but probably apply to other time-stepping algorithms.

B. Convergence due to machine accuracy and the size of the time step

Like many previous TDHF calculations, the first studies were performed using single-precision arithmetic on an IBM processor. By varying the time step, we found that physical convergence started for the smaller time steps, but at the same time certain sensitive numerical quantities deviated from their accepted accuracy. This behavior is demonstrated in the single-precision results shown in Figs. 6 and 7. Figure 6 shows the time dependence of the rms radius of the $^{86}Kr + {}^{139}La$ system at $E_{lab}=370$ MeV (the lowest energy studied), for Skyrme III with different time steps. The behavior of the solutions is clearly what one expects. From $\Delta t=0.01$ to $\Delta t=0.005$ (10^{-21} s) there is a drastic change from rapid reseparation to a more fusion-like collision. Decreasing Δt to 0.002 reproduces the same initial minimum as for $\Delta t=0.005$, but for later times the solutions remain noticeably different. Then for $\Delta t=0.001$ the rms radius is the same as for $\Delta t=0.002$ up to about $t=5\times10^{-21}$ s. Thus, based on the results for the two smallest time steps, we could conclude that the confidence time is about 5×10^{-21} s.

Also, calculations in double precision reproduce the results shown in Fig. 6. At this point, it appears then that convergence is established and that results computed with the smallest two time steps can be trusted up to the confidence time. However, by examining other quantities, we find that new troubles appear. In Fig. 7 we show the

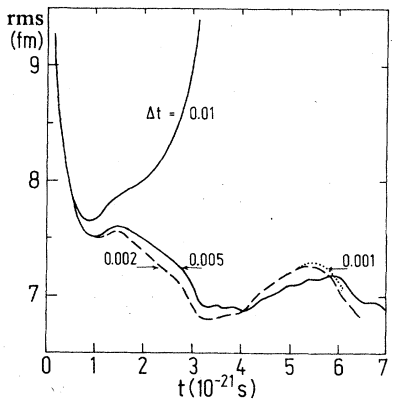

FIG. 6. The rms radius of the total system as a function of time for different time steps. The calculations are in single precision, for head-on collisions of $^{86}Kr + {}^{139}La$ at $E_{lab}=370.0$ MeV using the Skyrme III potential. The time steps are in units of 10^{-21} s. Calculations in double precision reproduce these results.

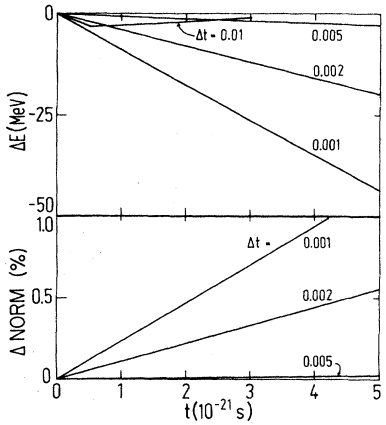

FIG. 7. The total energy and the single-particle norm as a function of time for different time steps in single precision calculations, for head-on collisions of $^{86}Kr + {}^{139}La$ at $E_{lab}=370.0$ MeV using the Skyrme III potential. The upper curve displays the change in the total energy. The lower curves plot the percentage deviation from unity of the highest occupied proton state; the behavior of this norm is typical of all other occupied single-particle states. The deviation of the norm for $\Delta t=0.01\times10^{-21}$ s is not shown since it can not be distinguished from the abscissa. The time steps are in units of 10^{-21} s.

change in the total energy and the percentage deviation from unity of the norm of one of the single particle wave functions as functions of time, again for different time steps. Clearly, while the rms radius appears to converge with Δt, the energy and norms deviate from their initial values as time proceeds and with discrepancies which get larger for the smaller time steps (which in principle should give greater accuracy). The obvious cause of this problem is round-off error. Looking at the algorithms appearing in the time integration, we find that there will typically be expressions like

$$\psi(t+\Delta t)=\psi(t)+\Delta t\dot{\psi} .$$

Since the floating point additions have a finite accuracy, an increasing number of digits of $\dot{\psi}$ will be lost in the addition as Δt get smaller. If the calculations for $\Delta t=0.002\times10^{-21}$ s are repeated in IBM double precision, the deviations in total energy and norm are practically eliminated. To summarize these results, we approximated both the total energy and the single-particle norm by linear functions,

$$E_{tot}(t)=E_{tot}(0)+at , \tag{A1}$$

$$||\psi||(t)=||\psi||(0)+bt , \tag{A2}$$

where the quantity $||\psi||$ is the norm of the single-particle state shown in Fig. 7. The resulting values for a and b are listed in Table IV.

In order to get an impression of the higher-energy behavior, another analysis was done with Skyrme IV at $E_{lab}=790.0$ MeV. Again a similar convergence pattern was obtained, but the confidence time decreased to about

TABLE IV. Fits to Eqs. (A1) and (A2) for studies of head-on collisions of $^{86}Kr + ^{139}La$ at $E_{lab} = 370.0$ MeV using the Skyrme III potential. The calculations were performed on the IBM 3033 at GSI. Note that for the quantity b we retain more significant figures in the double precision calculations than in the single precision calculations.

Time step (10^{-21} s)	Precision of the calculation	a (MeV/10^{-21} s)	b (10^{21}/s)
0.010	single	−0.891	−0.000 01
0.005	single	0.564	0.000 1
0.002	single	4.171	0.001 1
0.001	single	9.637	0.002 4
0.002	double	0.022	−0.000 000 5

1.5×10^{-21} s, which roughly coincides with the initial minimum of the rms radius. However, the differences between the smaller time steps corresponded to differences in the details of the oscillations of the nucleus, so that the question of fusion may not be as critical as for smaller energies. At any rate, for the fusion problem, one may conclude that for present numerical methods it may be meaningless to follow the calculations for much more than 5×10^{-21} s, particularly if reseparation occurs after such a time interval. Fusion or reseparation in TDHF studies is probably best determined on the basis of the initial one or two oscillations of the rms radius.

[1] J. R. Nix and A. J. Sierk, Phys. Rev. C **15**, 2072 (1977).
[2] W. J. Swiatecki, Phys. Scr. **24**, 113 (1981).
[3] W. J. Swiatecki, Nucl. Phys. **A376**, 275 (1982).
[4] S. Bjørnholm and W. J. Swiatecki, Nucl. Phys. **A391**, 471 (1982).
[5] H. Feldmeier, Institut für Kernphysik, Technische Hochscule Darmstadt Report ISSN-0720-8715, 1982, p. 26.
[6] K. T. R. Davies, A. J. Sierk, and J. R. Nix, Phys. Rev. C **28**, 679 (1982). This paper contains additional theoretical and experimental references relevant to dynamical fusion thresholds.
[7] J. R. Nix and A. J. Sierk, Proceedings of the International Conference on Theoretical Approaches to Heavy Ion Reaction Mechanisms, Paris, France, 1984.
[8] K. T. R. Davies and S. E. Koonin, Phys. Rev. C **23**, 2042 (1981). Comprehensive lists of TDHF references relevant to fusion behavior are found in the paper and in the review articles, see Refs. 9 and 10.
[9] J. W. Negele, Rev. Mod. Phys. **54**, 913 (1982).
[10] K. T. R. Davies, K. R. S. Devi, S. E. Koonin, and M. R. Strayer, in *Heavy Ion Science, Nuclear Science,* edited by D. A. Bromley (Plenum, New York, 1985), Vol. 3, p. 3.
[11] A. K. Dhar and B. S. Nilsson, Nucl. Phys. **A315**, 445 (1979).
[12] P. Bonche, K. T. R. Davies, B. Flanders, H. Flocard, B. Grammaticos, S. E. Koonin, S. J. Krieger, and M. S. Weiss, Phys. Rev. C **20**, 641 (1979).
[13] K. R. S. Devi, A. K. Dhar, and M. R. Strayer, Phys. Rev. C **23**, 2062 (1981).
[14] K. R. S. Devi, M. R. Strayer, J. M. Irvine, and K. T. R. Davies, Phys. Rev. C **23**, 1064 (1981).
[15] K. T. R. Davies, K. R. S. Devi, and M. R. Strayer, Phys. Rev. Lett. **44**, 23 (1980).
[16] K. T. R. Davies, K. R. S. Devi, and M. R. Strayer, Phys. Rev. C **24**, 2576 (1981).
[17] H. Stöcker, R. Y. Cusson, H. J. Lustig, A. Gobbi, J. Hahn, J. A. Maruhn, and W. Greiner, Z. Phys. A **306**, 235 (1982).
[18] A. K. Dhar, Phys. Rev. Lett. **50**, 478 (1983).
[19] J. R. Nix, Comments Nucl. Part. Phys. **12**, 13 (1983).
[20] K. T. R. Davies, A. J. Sierk, and J. R. Nix, in *Proceedings of the International Conference on Nuclear Physics with Heavy Ions, Stony Brook, New York, 1983,* edited by Peter Brown-Munzinger (Harwood, New York, 1984), p. 57.
[21] A. Lazzarini, H. Doubre, K. T. Lesko, V. Metag, A. Scamster, R. Vandenbosch, and W. Merryfield, Phys. Rev. C **24**, 309 (1981).
[22] P. Bonche, B. Grammaticos, and S. E. Koonin, Phys. Rev. C **17**, 1700 (1978).
[23] S. J. Krieger and K. T. R. Davies, Phys. Rev. C **18**, 2567 (1978).
[24] Y. M. Engel, D. M. Drink, K. Goeke, S. J. Krieger, and D. Vautherin, Nucl. Phys. **A249**, 215 (1975).
[25] K. T. R. Davies, K. R. S. Devi, and M. R. Strayer, Phys. Rev. C **20**, 1372 (1979).
[26] K. T. R. Davies, H. T. Feldmeier, H. Flocard, and M. S. Weiss, Phys. Rev. C **18**, 2631 (1978).
[27] D. Vautherin and D. M. Brink, Phys. Rev. C **5**, 626 (1972).
[28] M. Beiner, H. Flocard, Nguyen Van Giai, and P. Quentin, Nucl. Phys. **A238**, 29 (1975).
[29] J. W. Negele, S. E. Koonin, P. Möller, J. R. Nix, and A. J. Sierk, Phys. Rev. C **17**, 1098 (1978).
[30] P. Hoodbhoy and J. W. Negele, Nucl. Phys. **A288**, 23 (1977).
[31] J. W. Negele and D. Vautherin, Phys. Rev. C **5**, 1472 (1972).
[32] H. Krivine, J. Treiner, and O. Bohigas, Nucl. Phys. **A336**, 155 (1980).
[33] J. Bartel, P. Quentin, M. Brack, C. Guet, and H. B. Hakansson, Nucl. Phys. **A386**, 79 (1982).
[34] C. Y. Wong and K. T. R. Davies, Phys. Rev. C **28**, 240 (1983). This paper contains additional references to studies involving corrections to the mean-field approximation.
[35] R. Vandenbosch, M. P. Webb, P. Dyer, R. J. Pugh, R. Weisfield, T. D. Thomas, and M. S. Zisman, Phys. Rev. C **17**, 1672 (1978).
[36] S. E. Koonin, K. T. R. Davies, V. Maruhn-Rezwani, H. Feldmeier, S. J. Krieger, and J. W. Negele, Phys. Rev. C **15**, 1359 (1977).